Vol. 1 No. 11 DA
www.signaling-gateway.org/reports/v1/DA0011/DA0011.htm

Multiplexed Lipid Arrays of Anti-Immunoglobulin M–Induced Changes in the Glycerophospholipid Composition of WEHI-231 Cells

Stephen B. Milne, Jeffrey S. Forrester, Pavlina T. Ivanova, Michelle D. Armstrong, and H. Alex Brown
Alliance for Cellular Signaling Lipidomics Laboratory
Department of Pharmacology and the Institute for Chemical Biology, Vanderbilt University Medical Center, Nashville, TN

Abstract: A goal of the Alliance for Cellular Signaling (AfCS) is to identify the diverse participants that compose an intracellular signaling network. Phospholipids are important participants in transmembrane signaling processes as well as direct mediators of the dynamic aspects of cell membrane structure. Therefore, identifying the contextual changes in membrane lipid composition (in addition to that of genes and proteins) is essential in achieving a comprehensive understanding of signaling networks in cells. Recent advances in high-throughput electrospray ionization mass spectroscopy (ESI-MS) coupled with new computational approaches have greatly facilitated this goal. One cell type of interest to the AfCS is the splenic B lymphocyte and its experimental surrogate, the WEHI-231 cell (1, 2). Here we identify more than 200 species of glycerophospholipids from total membrane extracts of WEHI-231 cells and qualitatively measure pattern response changes initiated by stimulation of cell surface receptors.

In these studies, WEHI cells were treated with anti-immunoglobulin M antibody (AIG) to stimulate the B-cell receptor. The response to AIG stimulation was a conspicuous change in a broad range of phospholipids. An overall temporal trend was observed in which lipid concentration changes were detected by 6 minutes, pattern changes peaked by 15 minutes, and by 4 hours of stimulation, the cells had largely returned to their prestimulated composition. Statistically significant decreases were observed in many species of phospholipids along with concomitant increases in lysophospholipid concentrations. This study represents the most comprehensive analysis of membrane phospholipid changes in any cell type to date. The procedure described can be applied to any mammalian cell type and provides a basis for the comprehensive study of lipid signal transduction. Taken together, these changes form unique patterns that will be used to discriminate ligand-stimulated events and to model signaling pathways that lead to developmental and phenotypic changes in cells.

Glycerolipids and glycerophospholipids are key molecules in many inter- and intracellular signal transduction pathways. Some of these processes, such as the phospholipase C (PLC)-driven phosphatidylinositol cycle, have been known to participate in signal transduction since the 1950s (3). Phosphatidic acid (PA) and diacylglycerol (DAG) participate in signaling pathways initiated by growth factors and G protein-coupled receptors (GPCRs) as well. However, the importance of additional lipid classes as cellular signals has only more recently been appreciated. These include the participation of lysophosphatidic acid in apoptosis and lysophospholipids as ligands for certain GPCRs involved in cardiac, neuronal, and immunological processes (4-7).

Until recently, the detection and identification of low concentration lipids was quite difficult. Thin layer chromatography (TLC) was utilized for many decades to separate lipid classes. With the advent of gas chromatography and gas chromatography mass spectrometry (GC-MS), class separation by TLC followed by hydrolysis and derivatization made it possible to identify individual fatty acid species. One of the drawbacks to this method was that large amounts of lipids were normally required. With the introduction of fast atom bombardment mass spectrometry (FAB-MS), routine analysis of intact phospholipids was possible (8). More recently, electrospray ionization mass spectrometry (ESI-MS) has greatly simplified the procedures for lipid analysis. The soft ionization process associated with ESI-MS results in decreased molecular ion decomposition and lower detection limits compared to FAB-MS (9, 10).

A primary goal of these studies has been to identify the phospholipids participating in the cellular signaling pathways downstream of the AIG pathway in WEHI-231 cells as well as other ligands of interest to the AfCS. In this way, lipid signaling components can be integrated into the larger cellular signaling network, appreciated as part of the molecular response elements used by cells to transduce information from the cell surface, and better understood regarding the sometimes mysterious events occurring within cellular bilayers. As such, this report represents the most extensive analysis of cellular lipid content and changes determined to date. The ability to monitor changes in cellular lipid content in parallel with the ability of other AfCS laboratories to determine changes in gene expression, protein modifications, and production of second messengers represents a powerful new approach to understanding the contextual changes that determine cellular responses to complex biological stimuli.

Results

Identification of Lipids by Mass Spectrometry

Identification of the individual glycerophospholipids present in the total lipid extracts (both basal and AIG-stimulated) was accomplished by tandem mass spectrometry (ESI-MS/MS). Resolution and characterization of

glycerophospholipids in an unprocessed total lipid extract are based on the predisposition of each lipid class to acquire positive or negative charges under the source energy. A single molecular ion is present with a mass-to-charge ratio (*m/z)* that refers to the monoisotopic molecular weight. Collision-induced dissociation (CID) of the peaks of interest yielded fragmentation patterns, which were used to unambiguously identify the lipid(s) present at a particular *m/z* value (Fig. 1 provides an illustration of this procedure) (11-23).

For tandem mass spectrometry, both positive and negative mode ionization were utilized. Traditionally, degree of structural information obtained as a result of this analysis varies by the type of instrumentation used. In negative ionization mode, triple quadrupole instruments tend to yield

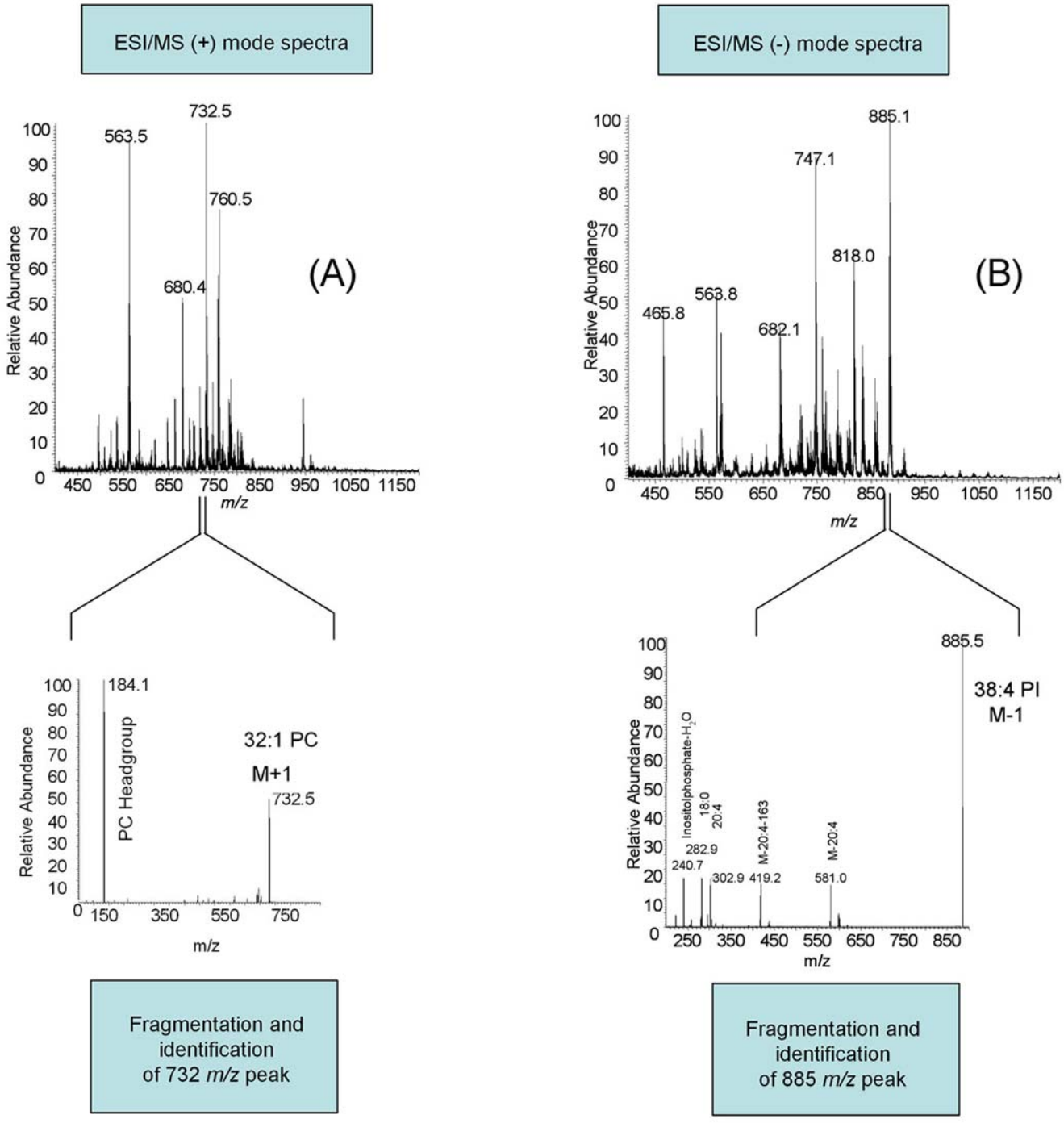

Fig. 1**. Fragmentation and identification of lipid species**. Individual lipid species from the total cell extract were isolated and fragmented using ESI-MS/MS. Positive mode analysis was utilized in the identification of three phospholipid classes. Negative mode analysis was used to assign five classes and to determine fatty acid compositions.

sn-1 and *sn*-2 fatty acid residue fragments, whereas ion traps form more lyso-lipid fragments (19). Positive ion ESI-MS/MS spectra from ion trap instruments are more likely to create lyso-PC fragmentation products, which reveal the fatty acid composition of the lipid. However, under our triple quadrupole MS experimental conditions, only glycerophospholipid head group information was routinely obtainable from positive mode fragmentation.

Three lipid classes were analyzed in positive ESI mode: phosphatidylcholines (PCs), phosphatidylethanolamines (PEs), and sphingomyelins (SMs). The choline containing species, PCs and SMs, both show a characteristic *m/z* 184 phosphocholine head group peak, as well as an $[M+H-59]^+$ peak corresponding to the neutral loss of $(CH_3)_3N$. In addition to the diacyl PC compounds, a large number of plasmanyl and plasmenyl phosphocholines were also identified. All together, over 100 choline containing lipids were identified. Fragmentation of phosphatidylethanolamines exclusively

Table 1. ***Fragmentation table for phosphatidylserines***. Using negative mode ESI-MS/MS, 33 PS and lyso-PS species were identified. The numbers in parentheses following fragment ions (FA:D) refer to the total number of fatty acid carbons (FA) and fatty acid carbon-carbon double bonds (D). GP= glycerophosphate.

m/z	Compound	Fragmentation Ions				
		PA-H	LPA-H_2O-H	LPA-H	Fatty Acid-H	GP-H_2O-H
706	30:0 PS	619	363 (14:0), 390 (16:0)		227 (14:0), 255 (16:0)	
730	32:2 PS	643	389 (16:1)	407 (16:1)	253 (16:1)	153
732	32:1 PS	645	389 (16:1), 391 (16:0)	407 (16:1), 409 (16:0)	253 (16:1), 255 (16:0)	
734	32:0 PS	647	391 (16:0)	409 (16:0)	255 (16:0)	153
756	34:3 PS	669	391 (16:0), 415 (18:2)	407 (16:1)	253 (16:1), 255 (16:1), 279 (18:2), 281 (18:1)	
758	34:2 PS	671	389 (16:1), 391 (16:0), 415 (18:2), 417 (18:1)	433 (18:2), 435 (18:1), 409 (16:0), 407 (16:1)	253 (16:1), 255 (16:0), 279 (18:2), 281 (18:1)	153
760	34:1 PS	673	389 (16:1), 391 (16:0), 417 (18:1), 419 (18:0)	435 (18:1), 437 (18:0)	253 (16:1), 255 (16:0), 281 (18:1), 283 (18:0)	
762	34:0 PS	675	391 (16:0), 419 (18:0)	437 (18:0)	255 (16:0), 283 (18:0)	153
782	36:4 PS	695	391 (16:0), 439 (20:4)	409 (16:0)	253 (16:1), 255 (16:0), 303 (20:4), 305 (20:3)	
784	36:3 PS	697	391 (16:0), 441 (20:3)	409 (16:0), 459 (20:3)	255 (16:0), 305 (20:3)	153
786	36:2 PS	699	415 (18:2), 417 (18:1), 419 (18:0)	433 (18:2), 435 (18:1), 437 (18:0)	279 (18:2), 281 (18:1), 283 (18:0)	153
788	36:1 PS	701	417 (18:1), 419 (18:0)	435 (18:1), 437 (18:0)	281 (18:1), 283 (18:0)	
790	36:0 PS	703	419 (18:0)	437 (18:0)	283 (18:0)	
806	38:6 PS	719	391 (16:0), 463 (22:6)	409 (16:0), 481 (22:6)	253 (16:1), 255 (16:0), 327 (22:6), 329 (22:5)	
808	38:5 PS	721	417 (18:1), 439 (20:4)	435 (18:1)	281 (18:1), 303 (20:4)	153
810	38:4 PS	723	417 (18:1), 419 (18:0), 439 (20:4), 441 (20:3)	435 (18:1), 437 (18:0), 457 (20:4)	281 (18:1), 283 (18:0), 303 (20:4), 305 (20:3)	153
812	38:3 PS	725	419 (18:0), 441 (20:3)	437 (18:0), 459 (20:3)	283 (18:0), 305 (20:3)	153
814	38:2 PS	727	419 (18:0), 443 (20:2)	437 (18:0), 461 (20:2)	283 (18:0), 307 (20:2)	153
816	38:1 PS	729	419 (18:0)		283 (18:0), 309 (20:1)	153
832	40:7 PS	745	417 (18:1), 463 (22:6)	435 (18:1), 481 (22:6)	281 (18:1), 327 (22:6)	
834	40:6 PS	747	417 (18:1), 419 (18:0), 463 (22:6), 465 (22:5)	435 (18:1), 437 (18:0), 481 (22:6)	279 (18:2), 281 (18:1), 283 (18:0), 327 (22:6), 329 (22:5), 331 (22:4)	153
836	40:5 PS	749	417 (18:1), 419 (18:0), 465 (22:5), 467 (22:4)	437 (18:0), 483 (22:5), 485 (22:4)	281 (18:1), 283 (18:0), 329 (22:5), 331 (22:4)	153
838	40:4 PS	751	419 (18:0), 467 (22:4)	437 (18:0)	283 (18:0), 331 (22:4)	153
494	16:1 LPS	407		407 (16:1)	253 (16:1)	153
496	16:0 LPS	409		409 (16:0)	255 (16:0)	153
522	18:1 LPS	435		435 (18:1)	281 (18:1)	153
524	18:0 LPS	437		437 (18:0)	283 (18:0)	153
544	20:4 LPS	457		457 (20:4)	303 (20:4)	153
546	20:3 LPS	459		459 (20:3)	305 (20:3)	
550	20:1 LPS	463		463 (20:1)	309 (20:1)	
568	22:6 LPS	481	463 (22:6)	481 (22:6)	327 (22:6)	153
570	22:5 LPS	483		483 (22:5)	329 (22:5)	153
572	22:4 LPS	485	467 (22:4)	485 (22:4)	331 (22:4)	153

yielded one peak, an $[M+H-141]^+$ ion from the neutral loss of the phosphoethanolamine head group. Again, plasmanyl and plasmenyl lipids were a large proportion of the over 40 PE species identified.

Five lipid classes were detected in negative ESI mode: phosphatidylinositiols (PIs), phosphatidylserines (PSs), phosphatidylglycerols (PGs), glycerophosphatidic acids (PAs), and PEs. Negative mode fragmentation of these species yielded a wealth of structural information. In each case, head group fragmentation, lyso-lipid formation, and fatty acid fragments aided in the lipid identification process. Phosphatidylinositol fragmentation generated a wide variety of product ("daughter") ions. Four types of lysophosphatidic acid and lysophosphatidylinositols, phosphatidic acid, and five characteristic head group fragments were used in identifying the 27 observed PI and lyso-PI species. In a similar fashion, 33 distinct species of PS and lyso-PS compounds were identified from their phosphatidic (PA) and lysophosphatidic acid (LPA) fragments. A negative mode fragmentation library of the phosphatidylserines is provided as an example in Table 1. Fragmentation tables for the remaining phospholipid classes (for both fragmentation modes) can be viewed online at http://www.signaling-gateway.org/reports/v1/DA0011/DA0011.htm. Phosphatidylcholine compounds were not identified during the routine negative mode scans. However, it was found that these compounds were detectable after the addition of ammonium acetate (15, 18, and 23). Two important categories of signaling lipids were not included in this analysis. Diacylglycerol (DAG) was not routinely detected under the optimized conditions for triple quadrupole MS described here; however, DAG species can be detected using a Fourier transform ion cyclotron resonance (FT-ICR) instrument (16). We have also found that DAG can be detected using a triple quadrupole MS but requires formation of a sodium adduct. In the current study, well over 200 glycerophospholipids have been detected and unambiguously identified in WEHI-231 total lipid extracts. A tabular listing of all identified lipids for both positive and negative MS modes is shown in Table 2.

Mathematical Analysis of Mass Spectrometry Data

Comprehensive Analysis of Lipid Changes under Stimulation. The goal of the computational analysis is the construction of an array containing the *m/z* ratios for peaks observed within a mass spectrometry experiment that displays the comprehensive changes in these species between two experimental conditions (e.g., addition of a ligand at a given concentration) over the defined time course. In order to accomplish this goal, computer algorithms were developed by our group to achieve the following: (i) smooth raw mass spectrometry data to remove extraneous portions; (ii) identify peaks within each data set and normalize their signal intensities; (iii) create baseline profiles of the transformed signal at each peak identified; (iv) statistically compare these baseline conditions with the observed stimulated results; and (v) handle exceptional cases in which assumptions are not validated by the data. All data analysis programs were written in the S-Plus V3.3 for Windows environment. These steps are outlined in Fig. 2.

The data analysis begins with the conversion of Xcalibur raw files into text for loading into S-Plus. After the files are loaded, each data set is smoothed using a kernel regression estimator (24). The effect of this smoothing is the removal of shoulders from peaks within the data set, which reduces the overall number of peaks to be analyzed. This smoothed data set is then transformed in the second portion of the analysis.

Since the absolute signal intensity at a particular *m/z* value exhibits a high variability, even between apparent exact replicates, the development of a unitless number was desirable for the comparison of this data. The primary characteristic for this transformation was that it should be a more robust measure of the signal strength at a particular *m/z* value with

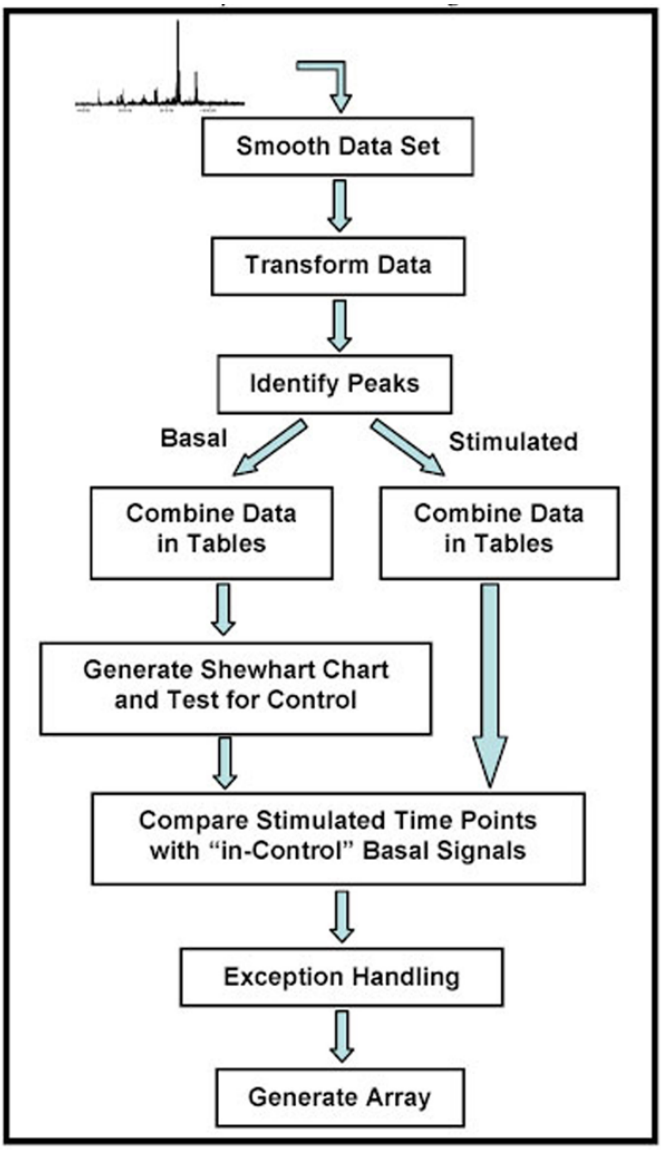

Fig. 2**. Flowchart for the analysis of mass spectrometry data in the creation of lipid arrays.**

Table 2. ***Library of identified glycerophospholipid species***. All of the glycerophospholipids identified by ESI-MS/MS fragmentation in positive and negative modes are summarized. PC and PE compounds with lower case e or p refer to plasmanyl and plasmenyl (alkyl ether and plasmalogen) subspecies, respectively. When plasmanyl and plasmenyl PE or PC species are separated by and/or (a/o), this indicates that one or both species were detected at that *m/z*.

m/z	Negative	Positive	*m/z*	Negative	Positive
409	16:0 LPA		754		34:4 PC, 38:3 PEp a/o 38:4 PEe
421	18:0_p LPA		756	34:3 PS	34:3 PC
424	14:0 LPE		758	34:2 PS	34:2 PC
437	18:0 LPA		760	34:1 PS	34:1 PC, 34:2 PS
440		12:0 LPC	762	34:0 PS, 38:6 PE	34:0 PC, 38:0 PEe
450	16:1 LPE		764	38:5 PE	38:6 PE
452	16:0 LPE	16:1 LPE	766	38:4 PE	38:5 PE, 36:4 PCp
454		16:0 LPE	768	38:3 PE	38:4 PE, 36:3 PCp a/o 36:4 PCe
455	14:0 LPG		769	36:4 PG	
466	16:0 PE std		770	38:2 PE	38:3 PE 36:2 PCp a/o 36:3 PCe
467	16:0 PE std		771	36:3 PG	
468		16:0 PE std, 14:0 LPC	772	38:1 PE	36:1 PCp a/o 36:2 PCe
469		16:0 PE std	773	36:2 PG	
478	18:1 LPE		774	40:6 PEp	36:0 PCp a/o 36:1 PCe
480	18:0 LPE	18:1 LPE	775	36:1 PG	
482		18:0 LPE	776	40:5 PEp a/o 40:6 PEe	36:0 PCe, 38:0 PE a/o 40:6 PEp
483	16:0 LPG		778		36:6 PC, 40:5 PEp a/o 40:6 PEe
494	16:1 LPS	16:1 LPC	780		36:5 PC
496	16:0 LPS	16:0 LPC	781	30:0 PI	
500	20:4 LPE		782	36:4 PS	36:4 PC
502	20:3 LPE		784	36:3 PS	36:3 PC
506		20:2 LPE	786	36:2 PS	36:2 PC, 40:1 PEp a/o 40:2 PEe
509	18:1 LPG		788	36:1 PS	36:1 PC
511	18:0 LPG		790	40:6 PE, 36:0 PS	40:0 PEe, 36:0 PC a/o 38:6 PCp
522	18:1 LPS	18:1 LPC	792	40:5 PE	40:6 PE, 38:5 PCp a/o 38:6 PCe
524	22:6 LPE, 18:0 LPS	18:0 LPC	794		40:5 PE, 38:4 PCp a/o 38:5 PCe
526	22:5 LPE		796		40:4 PE, 38:3 PCp a/o 38:4 PCe
536	d 18:1/16:0 Ceramide		797	38:4 PG	
544	20:4 LPS	20:4 LPC	798		38:2 PCp a/o 38:3 PCe
546	20:3 LPS	20:3 LPC			
548		20:2 LPC	800		38:1 PCp a/o 38:2 PCe
550	20:1 LPS	20:1 LPC	802		38:0 PCp a/o 38:1 PCe
552		20:0 LPC	804		38:0 PCe
568	22:6 LPS	22:6 LPC	805	32:2 PI	
569	16:1 LPI		806	38:6 PS	38:6 PC
570	22:5 LPS	22:5 LPC	807	32:1 PI	
571	16:0 LPI		808	38:5 PS	38:5 PC
572	22:4 LPS	22:4 LPC	809	32:0 PI	
580		22:0 LPC	810	38:4 PS	38:4 PC
597	18:1 LPI		812	38:3 PS	38:4 PS, 38:3 PC
599	18:0 LPI		814	38:2 PS	38:2 PC
619	20:4 LPI		816	38:1 PS	38:1 PC
621	20:3 LPI		818		40:6 PCp a/o 38:0 PC
636		26:0 PCe	820		40:5 PCp a/o 40:6 PCe
662	30:0 PE		822		40:4 PCp a/o 40:5 PCe
663			824		40:3 PCp a/o 40:4 PCe
664		28:0 PCe, 30:0 PE	826		40:2 PCp a/o 40:3 PCe
671	34:2 PA		828		40:1 PCp a/o 40:2 PCe
673	34:1 PA		830		40:0 PCp a/o 40:1 PCe
674	32:1 PEe a/o 32:0 PEp	32:1 PEp a/o 32:2 PEe	832	40:7 PS	40:0 PCe
676	32:0 PEe	28:1 PC, 32:1 PEe	833	34:2 PI	
678		32:0 PEe, 28:0 PC	834	40:6 PS	40:6 PC
686		30:2 PCp a/o 30:3 PCe	835	34:1 PI	
688	32:1 PE	32:2 PE, 30:1 PCp a/o 30:2 PCe	836	40:5 PS	40:5 PC

Table 2 Continued. ***Library of identified glycerophospholipid species.***

m/z	Negative	Positive	*m/z*	Negative	Positive
690	32:0 PE	32:1 PE, 30:0 PCp a/o 30:1 PCe	837	34:0 PI	
692		32:0 PE, 30:0 PCe	838	40:4 PS	40:4 PC
699	36:2 PA		840		40:3 PC
			842		40:2 PC
700		30:3 PC	844		40:1 PC
701	36:1 PA	d 18:1/16:1 SM	846		40:0 PC
702	34:0PEp a/o 34:1 PEe	30:2 PC	852		42:3 PCp a/o 42:4 PCe
703		d 18:1/16:0 SM	854		42:2 PCp a/o 42:3 PCe
704		30:1 PC, 34:0 PEp a/o 34:1 PEe	855	36:5 PI	
706	30:0 PS	30:0 PC	856		42:1 PCp a/o 42:2 PCe
712	34:3 PE	34:4 PE	857	36:4 PI	
714	34:2 PE	34:3 PE	858		42:0 PCp a/o 42:1 PCe
716	34:1 PE	34:2 PE, 32:1 PCp a/o 32:2 PCe	859	36:3 PI	
718	34:0 PE	34:1 PE, 32:0 PCp a/o 32:1 PCe	860		42:0 PCe
719	32:1 PG		861	36:2 PI	
720		32:0 PCe, 34:0 PE	863	36:1 PI	
721	32:0 PG, 38:5 PA		864		42:5 PC
722	36:4 PEp		865	36:0 PI	
723	38:4 PA		866		42:4 PC
724		36:4 PEp	868		42:3 PC
728	36:1 PEp a/o 36:2 PEe	32:3 PC, 36:2 PEp a/o 36:3 PEe	870		42:2 PC
730	32:2 PS, 36:0 PEp a/o 36:1 PEe	32:2 PC, 36:1 PEp a/o 36:2 PEe	872		42:1 PC
732	32:1 PS	32:1 PC, 36:0 PEp a/o 36:1 PEe	874		42:0 PC
734	32:0 PS	32:0 PC	880		44:1 PCp a/o 44:2 PCe
736	36:5 PE		881	38:6 PI	
738	36:4 PE	34:4 PCp, 36:5 PE	882		44:0 PCp a/o 44:1 PCe
740	36:3 PE	36:4 PE	883	38:5 PI	
742	36:2 PE	36:3 PE, 34:2 PCp a/o 34:3 PCe	884		44:0 PCe
744	36:1 PE	36:2 PE, 34:1 PCp a/o 34:2 PCe	885	38:4 PI	
745	34:2 PG		887	38:3 PI	
746	38:6 PEp	36:1 PE, 34:0 PCp a/o 34:1 PCe	889	38:2 PI	
747	34:1 PG		909	40:6 PI	
748	38:5 PEp	34:0 PCe	911	40:5 PI	
750	38:4 PEp	38:5 PEp a/o 38:6 PEe	913	40:4 PI	
752		34:5 PC, 38:4 PEp a/o 38:5 PEe			

respect to the overall pattern observed. Our software is set up for two distinct methods for transforming the data. In the first method, the mean and standard deviation of a function of the observed intensities for the complete spectra are calculated. These statistics are then used to transform the signal intensity at each of the *m/z* values as: I* = (I - mean)/ SD (i.e., the transformed intensity is represented as the number of standard deviations the signal occurs above or below the mean signal strength). Thus, a signal with intensity equal to the mean intensity of the data set would receive a score of zero, and any signal with intensity below the mean would receive a negative score. The second method involves using the rank of the signal in comparison with the other points in the data set as the transformed intensity. This method has proven to be highly robust against the wide changes in signal magnitude observed. These transformed intensity signals are carried into the next level of analysis.

After the data have been smoothed and transformed, the algorithm identifies potential peaks by parsing for low-high-low patterns in the data set. These peaks are collected and concatenated with other data sets from the same condition. During this concatenation, the algorithm averages the locations of peaks identified within different data sets to compensate for *m/z* measurement error. For example, peaks identified at *m/z* ratios of 768.4 and 768.6 are placed at 768.5 for the analysis.

In the next stage of the analysis, the data from the basal condition are used to create a Shewhart control chart for the means of the transformed data. The object of this construction is the identification of *m/z* ratios for which the signal remains stable in the basal condition during the course of the experiment so that the information can be pooled for subsequent comparison with the stimulated condition. In the analysis of the WEHI-231 cells, we have $n = 4$ samples at each time point. The mean of these values is plotted along the time axis and a set of control limits are calculated for this statistic. The area between these limits represents the expected variability in the mean of four observations of the process, not the individual measurements. The limits are computed from process output, assuming the underlying distribution remains stable. Thus, a kind of running hypothesis test is constructed. An example of this stage of the analysis

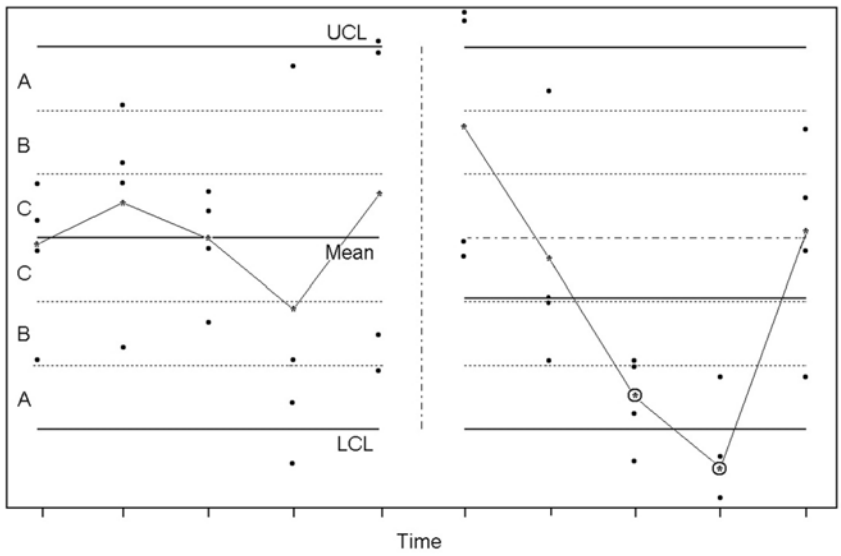

Fig. 3. **Shewhart control chart.** The left panel of the figure represents a control chart for the sample mean of the transformed data at a specific *m/z* value constructed from the basal case at five time points with four measurements each. The y-axis is unitless. The means of the sets are connected with a solid line. The chart also shows the grand mean as well as the lower and upper control limits, LCL and UCL, respectively. The area between the grand mean and the control limits is divided into zones labeled A, B, and C, as they proceed toward the center of the control chart. These zones represent the 3σ, 2σ, and 1σ distance from the grand mean and are used to test for time-dependent nonrandom patterns. The right panel of the figure shows the data for the stimulated condition, compared against the basal control limits, indicating an out-of-control condition at the third and fourth time points.

is shown in the left panel of Fig. 3.

A process is said to be "in control" if it exhibits only random variation, that is, all points (means in this case) are within the control limits and no nonrandom patterns are present. Our algorithm uses the zones labeled A, B, and C in the control chart to examine the time series for nonrandom patterns. At all *m/z* values at which the basal data remain in control over the course of the experiment, it is assumed that the variability in the signal output is appropriately represented by the control limits. These *m/z* values represent molecules in which metabolic cellular events are negligible, as measured by mass spectrometry, in the nonstimulated condition. An example of this can be seen in the left panel of Fig. 3, in which the signal denoted by the means of the four measurements is seen to be in control. In this case, these limits are used for comparison with the observed means at this *m/z* ratio in the stimulated condition, and these results are collected for processing into the lipid arrays. This analysis includes parsing for time points beyond the control limits as well as searching for patterns that can be deduced from the control chart zones. In Fig. 3, the third and fourth time points in the stimulated condition fail a nonrandom pattern test (two of three consecutive points in zone A or beyond; the fourth time point is beyond the lower control limit as well) and are flagged by the algorithm as having decreased in the stimulated condition.

The final portion of the computational analysis is the handling of exceptions to the above discussion. Two possibilities require elucidation here. In the first case, the basal data behave in an "out-of-control" manner, that is, they contain some nonrandom time-related variation. When the basal condition exhibits out-of-control variation, extending the control limits for comparison with the stimulated condition would be inappropriate. In this instance, a Welch-modified two-sample t-test is performed at each of the time points to determine if differences exist in the means between the two conditions at the given time. Thus, the algorithm performs an alternative statistical test at each time point for every *m/z* ratio in which the basal signal is found to be out of control. The second possibility involves peaks that appear in different frequencies within the basal and stimulated conditions. In this case, a binomial test is performed, with the null hypothesis that a peak has an equal chance of appearing in either of the two conditions, to determine if the observed difference in the number of occurrences in the two conditions is significant.

Lipid Arrays. At the conclusion of the analysis, the results are grouped into a comprehensive array containing the *m/z* values observed as peaks on the vertical and the time points on the horizontal axes. Lipid species that have been identified by CID MS/MS techniques as being present in the sample are assigned their corresponding *m/z* values. Each *m/z* and time point combination found to be increasing is scored with a one (1), while those decreasing are assigned a negative one (-1). Statistically stable combinations are scored with a zero (0). These arrays are color coded to enhance readability and in many cases provide a striking display of cellular lipid

Lipid	*m/z*		T1	T2	T3	T4	T5
38:4 PI	885.6		0	0	-1	-1	-1
	886.6		0	0	-1	-1	-1
38:3 PI	887.6		0	0	-1	-1	-1
	888.5		0	0	-1	-1	-1
38:2 PI	889.5		0	0	-1	-1	-1
	890.5		0	0	-1	-1	-1
38:1 PI	891.5		0	0	0	-1	0
	892.5		-1	1	-1	-1	-1

Fig. 4. **An excerpt from a lipid array in the *m/z* range of 885.6 to 892.5**. Data were collected from WEHI-231 cells challenged with 0.13 μM anti-IgM. Analysis using CID MS/MS determined that this area contained phosphatidylinositol lipids with 38 carbons in several double-bond configurations. The array shows these species decreasing over the time course after the stimulation, as indicated by the negative score.

changes in time after challenge with a biological agonist. An excerpt of a lipid array is shown in Fig. 4.

The number of peak/time point combinations examined in the system can create a significant opportunity for false-positives. This is illustrated by considering that if 1000 different peaks are analyzed over 5 time points, 5000 chances for a false-positive are created. If the alpha value is set at 0.05, one would anticipate 250 false indicators on a lipid array of this size occurring by chance alone. This effect can be countered by repeating the entire experiment multiple times and summing the cells from the resulting arrays. Thus, if the experiment is repeated five times, each cell in the summary array will have a score between -5 and 5. Scores occurring toward the extremes (-5 and 5) indicate species that are fluctuating under stimulation with high statistical significance. Since random errors are unlikely to occur in the same position, after several repetitions the result is seen to converge to a stable map of lipid changes.

Glycerophospholipid Changes in Basal Versus AIG-Stimulated WEHI-231 Cells

Stimulation of the AfCS WEHI-231 B-cell receptor with 0.13 µM anti-IgM ligand resulted in robust changes in glycerophospholipid concentrations. Lipid arrays were constructed from 10 sets of samples. Each data set contained four exact replicates of paired samples that included a control (basal) and matched ligand-stimulated sample at each of five time points: 1.5, 3, 6, 15, and 240 minutes. Thus, each array was constructed from 400 samples. The lipid species were identified using both the positive (array 1, supplemental material) and negative (array 2, supplemental material) ESI modes. Excerpts from the positive (A) and negative (B) mode arrays are shown in Fig. 5.

In array one, only a few changes in concentration were observed during the 1.5- and 3-minute time points. However, highly significant decreases were observed for many phosphatidylcholine and/or phosphatidylethanolamine species at the 6- and 15-minute time points, with corresponding increases in several lyso-PC compounds. By the fourth hour, the cells had mostly returned to their prestimulated states. A list of lipids having significant or highly significant changes is summarized in Table 3.

The temporal trend in array two was shifted towards the later time points. Little movement was observed during the 1.5-, 3-, or 6-minute experiments. But, clusters of phosphatidylinositols and phosphatidylserines were observed to decrease highly significantly at the 15-minute time point. Corresponding increases in lyso-PI, lyso-PS, and glycerophosphatidic acids were also recorded. A summary of observed changes for the entire array is shown in Table 4.

A

Lipid	*m/z*	1.5 min	3 min	6 min	15 min	240 min
	699.5	0	0	0	2	2
30:3 PC	700.6	-3	-1	-3	-5	-1
16:1 SM	701.5	3	-1	4	5	2
30:2 PC	702.6	0	0	2	2	-1
16:0 SM	703.6	-5	-2	-6	-9	-5

B

Lipid	*m/z*	1.5 min	3 min	6 min	15 min	240 min
	854.5	-2	-1	-2	-3	-1
36:5 PI	855.5	-1	-4	-3	-7	-5
	856.5	-3	-1	-4	-5	-3
36:4 PI	857.5	-1	-3	-3	-5	2
	858.5	-2	-4	-4	-7	1
36:3 PI	859.5	-2	-4	-3	-7	-4
	860.5	-2	-1	-3	-5	-4
36:2 PI	861.5	-2	-3	-5	-6	-5
	862.5	-3	-4	-2	-6	-4
36:1 PI	863.5	0	-2	-2	-3	0
	864.5	-3	-4	-4	-6	-1
36:0 PI	865.6	-3	-7	-5	-9	-1

Significance Key

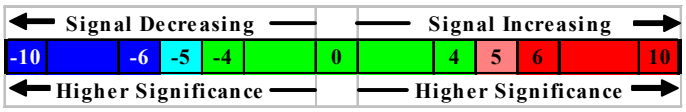

Fig. 5. **Excerpts from positive (A) and negative (B) mode lipid arrays**. The first column contains lipid species identified by ESI MS/MS. The second column indicates the mass-to-charge ratio (*m/z*) of the observed compounds. The remaining five columns are for the five time points (1.5, 3, 6, 15, and 240 minutes). The values in these columns represent the significance score, which is the sum of that cell for the 10 individual experiments, with positive numbers representing increasing signal and negative values indicating a decreasing signal. Therefore, an array cell containing the number -8 is interpreted to mean the indicated species was observed to decrease in 8 of the 10 trials and remain stable in the other 2, or that the species decreased in 9 of the experiments and increased in 1 at that time point. These scores are color coded by signal frequency with deep blue or red, indicating an absolute score of 6 or more from a possible 10 (shown highly significant by computer simulation). Lighter shades of red and blue indicate significant stimulations (-5 or 5). Green colored cells, representing a -4 to 4 significance score, indicate statistical stability between basal and stimulated conditions.

Table 3. ***Summary of glycerophospholipid changes following AIG stimulation of WEHI-231 cells (positive mode).***

POS		Time = 1.5 min		Time = 3 min		Time = 6 min		Time = 15 min			Time = 240 min	
Highly Significant	Decreasing					16:0 SM	36:0 PCp 36:1 PCe	16:0 SM	40:2 PCp 40:3 PCe	28:1 PC 32:1 PEe		
						36:2 PE 34:1 PCp 34:2 PCe	36:1 PCp 36:2 PCe	34:2 PE 32:1 PCp 32:2 PCe	40:3 PCp 40:4 PCe	36:0 PCp 36:1 PCe		
						28:1 PC 32:1 PEe	40:2 PCp 40:3 PCe	34:0 PC 38:0 PEe	40:5 PCp 40:6 PCe	36:1 PCp 36:2 PCe		
						36:1 PE 34:0 PCp 34:1 PCe	40:3 PCp 40:4 PCe	36:1 PE 34:0 PCp 34:1 PCe	40:4 PE 38:3 PCp 38:4 PCe	38:1 PCp 38:2 PCe		
						36:4 PC	38:4 PC	32:2 PC 36:1 PEp 36:2 PEe	36:0 PCe 38:0 PE 40:6 PEp	36:2 PE 34:1 PCp 34:2 PCe		
								30:1 PC 34:0 PEp 34:1 PEe	36:2 PC 40:1 PEp 40:2 PEe	34:1 PE		
								34:3 PC	36:4 PC	36:1 PC		
								34:2 PC	38:6 PC	40:6 PC		
								34:0 PCe	38:0 PCe			
	Increasing							20:0 LPC	20:1 LPC			
Significant	Decreasing	32:1 PE 30:0 PCp 30:1 PCe	36:1 PE 34:0 PCp 34:1 PCe	40:2 PCp 40:3 PCe		32:1 PE 30:0 PCp 30:1 PCe	32:2 PC 36:1 PEp 36:2 PEe	40:6 PCp 38:0 PC	32:0 PCe 34:0 PE	34:1 PC 34:2 PS	36:2 PE 34:1 PCp 34:2 PCe	36:6 PC 40:5 PEp 40:6 PEe
						38:1 PCp 38:2 PCe	38:3 PE 36:2 PCp 36:3 PCe	38:2 PCp 38:3 PCe	32:1 PE 30:0 PCp 30:1 PCe	38:3 PE 36:2 PCp 36:3 PCe	36:2 PC 40:1 PCp 40:2 PEe	
						30:1 PC 34:0 PEp 34:1 PEe	40:4 PE 38:3 PCp 38:4 PCe	40:0 PEe 36:0 PC 38:6 PCp	32:1 PC 36:0 PEp 36:1 PEe	32:0 PE 30:0 PCe	42:1 PCp 42:2 PCe	
						34:2 PC	38:5 PC	30:0 PC	36:3 PC	38:6 PE	40:6 PC	
		16:0 SM				36:3 PC	40:0 PC	30:3 PC	38:1 PC	36:5 PC	16:0 SM	
						36:2 PC 40:1 PEp 40:2 PEe		44:1 PCp 44:2 PCe	42:3 PCp 42:4 PCp	42:0 PCp 42:1 PCe	44:1 PCp 44:2 PCe	
								40:4 PC	40:0 PC	44:0 PCe		
									24:0 SM			
	Increasing	20:1 LPC						16:1 SM			20:0 LPC	

Table 4. ***Summary of glycerophospholipid changes following AIG stimulation of WEHI-231 cells (negative mode).***

NEG		Time = 1.5 min		Time = 3 min		Time = 6 min		Time = 15 min		Time = 240 min	
Highly Significant	Decreasing			36:0 PI				34:2 PI	36:3 PS	38:6 PI	
								36:0 PI	36:4 PS	40:6 PI	
								36:2 PI	38:4 PS		
								36:3 PI			
								36:5 PI			
								38:6 PI			
								40:6 PI	36:4 PG		
	Increasing							20:1 LPS		16:0 LPA	
Significant	Decreasing	40:6 PS				34:2 PI		36:4 PI	32:0 PS	34:2 PI	40:6 PS
						36:0 PI		38:4 PI	38:2 PS	36:2 PI	40:7 PS
						36:2 PI			40:6 PS	36:5 PI	
						38:4 PI					
						40:6 PS		32:1 PG	38:2 PE		
								34:1 PG	36:5 PE		
	Increasing							14:0 LPE		20:4 LPI	30:0 PA
								16:1 LPE			34:1 PA
								16:0 LPA	22:6 LPS	16:0 LPE	
								18:0p LPA			

Discussion

Anti-immunoglobulin (0.13 µM) stimulation of WEHI-231 cells resulted in a unique pattern of increasing and decreasing levels of glycerophospholipids. A wide variety of phosphatidylinositols, phosphatidylglycerols, and phosphatidylcholines decreased in concentration during the 6- and 15-minute time points, with corresponding increases in lysophospholipid levels. By the fourth hour, the GPL levels had essentially returned to their prestimulated states.

Due to detection limitations using triple quadrupole MS, diacylglycerols (DAGs) were not routinely analyzed in this study. Under our current experimental conditions, it is not possible to scan for DAGs and the remaining lipid classes simultaneously. In the future, samples will be split and changes in DAG levels will be monitored using an alternative procedure. Preliminary analysis measuring polyphosphoinositide levels is already underway and will be described in a subsequent report. The current methodology appears to be effective but cannot be run in parallel with other phospholipids. Detection of these species will almost certainly require multiple extractions and or separation by HPLC.

Mapping comprehensive lipid changes in time is thought to have many positive applications in cellular biology and cellular signaling. It is believed that data of this type will prove useful in hierarchical clustering schemes as another method in differentiating receptor-mediated cellular events involving lipid second messengers as well as membrane compositional remodeling. It is further believed that these arrays form a fingerprint that can be used to identify specific cellular responses and as such may prove useful in diagnostic profiling and elucidating lipid product-substrate relationships.

Methods and Protocols

Cell Extraction and Reconstitution

Phospholipids were extracted using a modified Bligh and Dyer procedure (25). Pellets containing 3 x 10^6 cells were extracted with 800 µL of 0.1 N HCl: MeOH (1:1) and 400 µL $CHCl_3$. The samples were vortexed (1 min) and centrifuged (5 min, 18,000 g). The lower phase was then isolated and evaporated (Labconco CentriVap Concentrator, Kansas City, MO), followed by reconstitution with 80 µL MeOH: $CHCl_3$ (9:1). Prior to analysis, 1 µL of NH_4OH was added to each sample to ensure protonation. Lipid standards were obtained from Avanti Polar Lipids (Alabaster, AL).

Mass Spectrometry Analysis of Phospholipid Cell Extracts

Mass spectral analysis was performed on a Finnigan TSQ Quantum triple quadrupole mass spectrometer (ThermoFinnigan, San Jose, CA) equipped with a Harvard Apparatus syringe pump and an electrospray source. Samples were analyzed at an infusion rate of 10 µL/min in both positive and negative modes over the range of *m/z* 400 to 1200. Instrument parameters were optimized with 1, 2-

dioctanoyl-*sn*-glycero-3-phosphoethanolamine (16:0 PE). Data were collected with the Xcalibur software package (ThermoFinnigan) and analyzed by a software program developed in our research group.

References

1. Gilman AG, Simon MI, Bourne HR, et al. (2002) Nature 420(6916), 703-706.
2. Sambrano GR, Chandy G, Choi S, et al. (2002) Nature 420(6916), 708-710.
3. Hokin LE. (1985) Annu. Rev. Biochem. 54, 205-235.
4. Hla T, Lee MJ, Ancellin N, Paik JH, and Kluk MJ. (2001) Science 294(5548), 1875-1878.
5. Pagès C, Simon M-F, Valet P, and Saulnier-Blache JS. (2001) Prostaglandins Other Lipid Mediat. 64(1-4), 1-10.
6. Goetzl EJ. (2001) Prostaglandins Other Lipid Mediat. 64(1-4), 11-20.
7. Fukushima N and Chun J. (2001) Prostaglandins Other Lipid Mediat. 64(1-4), 21-32.
8. Clay KL, Wahlin L, and Murphy RC. (1983) Biomed. Mass Spectrom. 10, 489-494.
9. Han X and Gross RW. (1994) Proc. Natl. Acad. Sci. U.S.A. 91(22), 10635-10639.
10. Kim HY, Wang TC, and Ma YC. (1994) Anal. Chem. 66(22), 3977-3982.
11. Kerwin JL, Tuininga AR, and Ericsson LH. (1994) J. Lipid Res. 35(6), 1102-1114.
12. Han X and Gross RW. (1995) J. Am. Soc. Mass Spectrom. 6, 1202-1210.
13. Han X and Gross RW. (1996) J. Am. Chem. Soc. 118, 451-457.
14. Brügger B, Erben G, Sandhoff R, Wieland FT, and Lehmann WD. (1997) Proc. Natl. Acad. Sci. U.S.A. 94(6), 2339-2344.
15. Fridriksson EK, Shipkova PK, Sheets ED, Holowka D, Baird B, and McLafferty FW. (1999) Biochemistry 38(25), 8056-8063.
16. Ivanova PT, Cerda BA, Horn DM, Cohen JS, McLafferty FW, and Brown HA. (2001) Proc. Natl. Acad. Sci. U.S.A. 98(13), 7152-7157.
17. Khaselev N and Murphy RC. (2000) J. Am. Soc. Mass Spectrom. 11(4), 283-291.
18. Murphy RC, Fiedler J, and Hevko J. (2001) Chem. Rev. 101(2), 479-526.
19. Larsen A, Uran S, Jacobsen PB, and Skotland T. (2001) Rapid Commun. Mass Spectrom. 15(24), 2393-2398.
20. Murphy RC. (2002) Mass Spectrometry of Phospholipids: Tables of Molecular and Product Ions. Denver, Colo: Illuminati Press.
21. Christie WW. (2003) Lipid Analysis: Isolation, Separation, Identification, and Structural Analysis of Lipids. Bridgwater, England: Oily Press.
22. Hsu FF and Turk J. (2003) J. Am. Soc. Mass Spectrom. 14(4), 352-363.
23. Pulfer M and Murphy RC. (2003) Mass Spectrom. Rev. 22(5), 332-364.
25. Bligh EG and Dyer WJ. (1959) Can. J. Biochem. Physiol. 37, 911-917.
24. Venables WN and Ripley BD. (1994) Modern Applied Statistics with S-Plus. New York, NY: Springer-Verlag.

Supplemental Tables

Table A	PA Negative Mode
Table B	PE Negative Mode
Table C	PG Negative Mode
Table D	PI Negative Mode
Table E	PE Positive Mode
Table F	PC Positive Mode
Array 1	WEHI IgM Positive Array
Array 2	WEHI IgM Negative Array

Authors*

H. Alex Brown†

Stephen B. Milne

Jeffrey S. Forrester

Pavlina T. Ivanova

Michelle D. Armstrong

Editors

Ashley K. Butler
Duke University, Durham, NC

Gilberto R. Sambrano‡
University of California San Francisco, San Francisco, CA

Reviewers

Lewis Cantley
Harvard Medical School, Boston, MA

* Please refer to the AfCS policy on authorship.
† To whom scientific correspondence should be addressed.
‡ To whom questions or comments about the AfCS Research Reports should be addressed.